

Static and Dynamic Behavior of Novel Y-Shaped Sandwich Beams Subjected to Compressive Loadings: Integration of Supervised Learning and Experimentation

Ali Khalvandi, Saeed Kamarian,* Mahdi Bodaghi, Saeed Saber-Samandari, and Jung-il Song*

In this article, an in-depth investigation into the mechanical response of novel Y-shaped core sandwich beams under static and dynamic compressive loading conditions is presented. Utilizing deep feed-forward neural networks (DFNNs) as the primary supervised learning scheme, the compressive behavior of these advanced structures is predicted. The trained DFNN model demonstrates high fidelity in capturing the stress–strain relationships, as evidenced by the close alignment of predicted and experimental results. Key design parameters of the cores of the sandwich beams are varied to understand their influence on the beams' linear, plateau, and densification regions, where higher values of design parameters contribute to increased stiffness, prolonged plateau regions, and higher densification points. Additionally, the impact of loading rates (1, 7, and 14 mm min⁻¹) on the mechanical performance is analyzed, revealing significant rate-dependent behaviors. The decision tree algorithm exhibits superior classification performance with a 99.79% accuracy, further validating the robustness of the predictive model. In contrast, the support vector machine algorithm with radial basis function shows moderate accuracy at 75.12%. Through these findings, the potential of DFNNs in predictive modeling and the importance of design parameters and loading rates in optimizing the mechanical performance of novel Y-shaped core sandwich beams is proposed.

civil engineering due to their high strength-to-weight ratio, excellent energy absorption, and superior thermal insulation properties.^[3] The outer layers, often made from materials such as metals or fiber-reinforced polymers, provide high stiffness and strength, while the core, typically made from lightweight materials like foam or honeycomb, offers shear resistance and helps in distributing loads.^[4–7] The innovative design and material selection of sandwich beams, a specific type of sandwich structures, enable their application in scenarios where both lightweight and high performance are critical.^[8–10] This article focuses on the study of sandwich beams fabricated using 3D-printing methods, specifically fused deposition modeling (FDM), which introduces new possibilities in terms of design complexity and material efficiency.

The fabrication of sandwich beams can be achieved through various methods including traditional techniques such as hand layup, resin transfer molding, and more advanced methods like additive


manufacturing (3D printing).^[11–13] Among these, 3D printing, particularly FDM, stands out due to its ability to create complex geometries with high precision and material efficiency. FDM works by extruding thermoplastic filaments layer by layer to build up the desired structure. This method allows for customization in the design of the core geometry, which is crucial for

1. Introduction

Sandwich structures are a class of engineering structures that consist of two thin layers on their both top and bottom, strong outer layers bonded to a lightweight, and a thick core.^[1,2] These configurations are widely used in aerospace, automotive, and

A. Khalvandi, S. Saber-Samandari
Composites Research Laboratory (CRLab)
Amirkabir University of Technology
Tehran 1591634653, Iran

A. Khalvandi, S. Saber-Samandari
New Technologies Research Center
Amirkabir University of Technology
Tehran 1591634653, Iran

 The ORCID identification number(s) for the author(s) of this article can be found under <https://doi.org/10.1002/adem.202402157>.

S. Kamarian, J. Song
The Research Institute of Mechatronics
Changwon National University
Changwon 51140, South Korea
E-mail: kamarian@changwon.ac.kr; jisong@changwon.ac.kr

© 2024 The Author(s). Advanced Engineering Materials published by Wiley-VCH GmbH. This is an open access article under the terms of the Creative Commons Attribution License, which permits use, distribution and reproduction in any medium, provided the original work is properly cited.

M. Bodaghi
Department of Engineering
School of Science and Technology
Nottingham Trent University
Nottingham NG11 8NS, UK

DOI: 10.1002/adem.202402157

optimizing the mechanical performance of sandwich beams.^[14] Additionally, FDM enables the use of a variety of thermoplastic materials, each offering different mechanical properties.^[15,16] In this study, we leverage the flexibility of FDM to fabricate sandwich beams with various symmetric core shapes. This approach not enhances the structural performance and provides insights into the relationship between core geometry and mechanical behavior under compressive loads.

When it comes to reviewing the published papers in the field, extensive research has been conducted on the design and performance of sandwich beams with different core configurations. Traditional core designs include honeycomb, foam, and truss structures, each offering unique advantages in terms of stiffness, strength, and weight.^[17–20] Recent studies have explored more complex core geometries to further optimize the mechanical properties of sandwich beams. Specifically, Y-shaped cores have garnered significant attention due to their potential to enhance load distribution and energy absorption. However, the effects of various symmetric core shapes on the compressive performance of sandwich beams remain underexplored. This article aims to fill this gap by investigating the compressive behavior of sandwich beams with different symmetric core shapes fabricated using FDM. Our study introduces a novel aspect by focusing on symmetric cores and examining their influence on the stress–strain response, providing valuable insights for the design of high-performance sandwich structures.

Accordingly, one approach by which the performance of sandwich beams can be analyzed is monitoring the compressive response of sandwich beams, involving both experimental and computational methodologies.^[21,22] Traditionally, compressive tests are conducted to obtain stress–strain curves, which provide essential information on the material behavior under load.^[23–25] However, with advancements in computational methods, machine learning (ML) techniques have become increasingly popular for predicting mechanical responses, specifically supervised learning approaches such as regression algorithms or classification methodologies. For instance, this study could benefit from implementing deep feed-forward neural networks (DFNNs) to simulate the compressive response of sandwich beams with different core geometries. DFNNs are a type of artificial neural network that excel in pattern recognition and predictive analysis, making them suitable for modeling complex mechanical behaviors.^[26,27] By training the FNN on experimental data, we can predict the stress–strain response of various core configurations with high accuracy can be predicted. This approach reduces the need for extensive physical testing and provides a deeper understanding of the relationship between core geometry and compressive performance. From another view, ML offers robust regression schemes to forecast complex phenomena with high accuracy.^[28–31] Specifically, ML-oriented regression methods are instrumental in predicting the mechanical properties of 3D-printed sandwich beams, a critical component in modern engineering applications.^[32] These regression models aim to identify patterns and predict outcomes under various loading conditions, thereby optimizing the design and performance of these structures.^[33–35] Complementarily, classification methods in ML are considerable in categorizing the behavior of sandwich beams and materials into distinct classes.^[36–38] This categorization facilitates understanding of

their response to different stressors, enabling engineers to tailor material properties and structural configurations for enhanced resilience and efficiency. Integrating regression and classification techniques thus provides a comprehensive framework for advancing the study and application of 3D-printed sandwich beams.

In this article, we present a comprehensive study on the fabrication and analysis of sandwich beams with novel symmetric Y-shaped cores using FDM 3D-printing method. The research begins by detailing the design and 3D-printing process for sandwich beams with various core geometries. Subsequently, uniaxial compressive tests are conducted to obtain experimental stress–strain curves for each core configuration. To enhance predictive accuracy, DFNNs are implemented to forecast the compressive behavior based on the experimental data. Other than the novel geometry of the beams, another new aspect of this study is where first ML-oriented regression is employed to predict the mechanical properties of the beams and second classification algorithms are utilized to categorize the beams' mechanical behavior based on the loading conditions (i.e., static and dynamic). This dual approach of using regression and classification schemes can lead to a detailed understanding of the beams' performance and elaborates on the potential of ML in structural sciences. The findings of this study offer new schemes for the design of sandwich structures with optimized mechanical properties, demonstrating the advantages of integrating 3D printing with advanced predictive modeling techniques such as prediction of the structures' responses and classifying them, which has been less under scrutiny.

2. Experimental Section

Using Design Expert software, the sandwich beams shown in **Figure 1** with innovative symmetric Y-shaped cores were designed utilizing a custom method, by which four design parameters at four levels were considered, resulting in 25 unique beam configurations. Throughout this design process, the length, height, and thickness of the face sheets were held constant to ensure consistency in the structural parameters. Specifically, the beams had a length of 160 mm and a width of 20 mm, with a total height of 140 mm. The height of the cores was fixed at 36 mm, and each face sheet had a thickness of 2 mm. Refer to **Figure 1** and **2** for detailed dimensions and configurations. Subsequently, the fabrication of these beams was undertaken using an FDM 3D printer, a common method for additive manufacturing that allows for precise control over the printing process. For this process, 1.75 mm diameter white polylactic acid (PLA+) filaments were selected as the primary material due to their favorable mechanical properties and ease of use.^[14] These filaments were fed into a BRIDE + FDM 3D printer provided by QUANTUM 3D. The printing parameters were chosen based on a specified protocol to optimize the quality and structural integrity of the beams. The nozzle temperature was set at 215 °C, which is optimal for PLA+ filament to ensure smooth extrusion and strong layer adhesion. The printer bed was maintained at 70 °C to minimize warping and ensure a stable base during the printing process. The printing speed was set to 50 mm min⁻¹, a balanced speed that ensured an appropriate

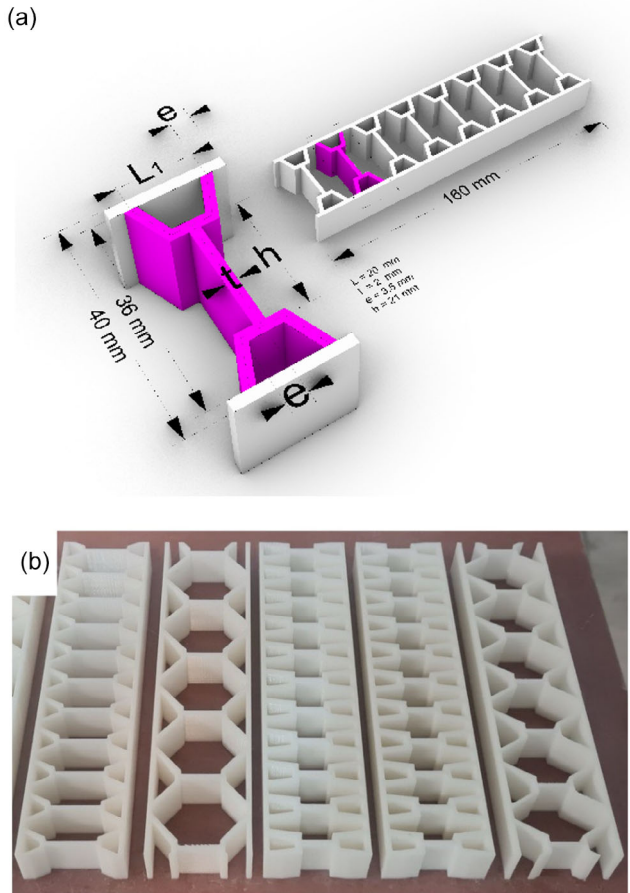


Figure 1. a) Layout of the designed sandwich beams, in which the key design parameters of the innovative symmetric Y-shaped core sandwich beams (i.e., L_1 , t , e , and h) are shown. The beams are 160 mm in total length, with a consistent width of 40 mm. b) The 3D-printed sandwich beams.

compromise between printing time and detail accuracy. Additionally, the layer height of 0.15 mm was chosen to produce fine, detailed layers that enhanced the overall mechanical properties of the printed beams, see **Table 1**.

To evaluate the performance of the novel Y-shaped core beams under various loading conditions, uniaxial compressive tests were conducted. These tests were designed to assess the behavior of the beams under both static and dynamic conditions. For the static tests, a crosshead speed of 1 mm min^{-1} was used to simulate a gradual application of load. For the dynamic tests, higher crosshead speeds of 7 and 14 mm min^{-1} were employed to simulate more rapid loading conditions. All the tests were carried out in the room temperature of $25 \text{ }^\circ\text{C}$, utilizing the SANTAM STM-50 universal testing machine equipped with a 50 kN loadcell provided by BONGSHIN (i.e., the DBBP-5t), based on the two solid-founded standards in the case of compressive testing of cellular structures, which were ISO 133 314:2011 and ASTM D1621.^[14] It is noteworthy that the tests were continued up to the state, at which the beams became fully dense and no more compressive deformations were experienced by the beams. These tests provided critical data on the mechanical

response and properties of the beams, contributing to a comprehensive understanding of their behavior under different scenarios.

3. Supervised Learning

In this section, elaborates on the supervised learning methodologies employed to predict the compressive responses of novel symmetric Y-shaped core sandwich beams. Our approach encompasses two primary supervised learning schemes: the implementation of DFNNs and the integration of ML-oriented regression and classification models. The DFNNs were utilized to forecast the stress–strain diagrams of the beams based on their design parameters and loading conditions. Subsequently, a combined regression and classification model approach was adopted to further elucidate the beams’ mechanical properties and classify their responses under static and dynamic loading scenarios. This comprehensive examination provides a robust framework for understanding and predicting the performance of these innovative structural elements, implementing advanced ML techniques to enhance accuracy and reliability.

3.1. DFNNs

In this study, DFNNs were implemented as the first supervised learning scheme to predict the compressive response of novel symmetric Y-shaped core sandwich beams. Six parameters were selected as the inputs for the DFNNs, which included the design parameters of the beams (i.e., L_1 , t , e , and h), all measured in millimeters. Additionally, the adopted loading crosshead speeds (1 , 7 , and 14 mm min^{-1}) and the induced compressive displacement during the tests (in mm) were also considered as inputs. The outputs were the compressive stress and strain values. Subsequently, a three-layer architecture was developed for the DFNNs’ hidden layers, with varying numbers of neurons in each layer determined through a trial-and-error process. The first hidden layer comprised 128 neurons, the second hidden layer had 64 neurons, and the third hidden layer contained 32 neurons, see **Figure 3**. The Levenberg–Marquardt algorithm was employed as the learning rule for the neural network due to its efficiency and accuracy in training complex models. The dataset was split into three parts: 70% was used for training, 15% for validation, and the remaining 15% for testing. This allocation ensured a robust evaluation of the network’s performance. Also, the learning rate was set to 0.001, a parameter carefully chosen to balance the convergence speed and the stability of the training process. Finally, to assess the performance of the deep neural networks, various metrics were calculated, including the absolute error (AE), mean absolute error (MAE), mean squared error (MSE), and the coefficient of determination (R^2), see Equation (1–4), in which X stands for the parameters that are to be predicted (i.e., strain and stress), and n is the number of data point. These metrics were crucial in evaluating the accuracy and reliability of the predictions made by the neural network. The goal was to ensure that the network accurately predicted the compressive response without overfitting, thus providing a reliable tool for understanding and the compressive behavior of the Y-shaped core sandwich beams.

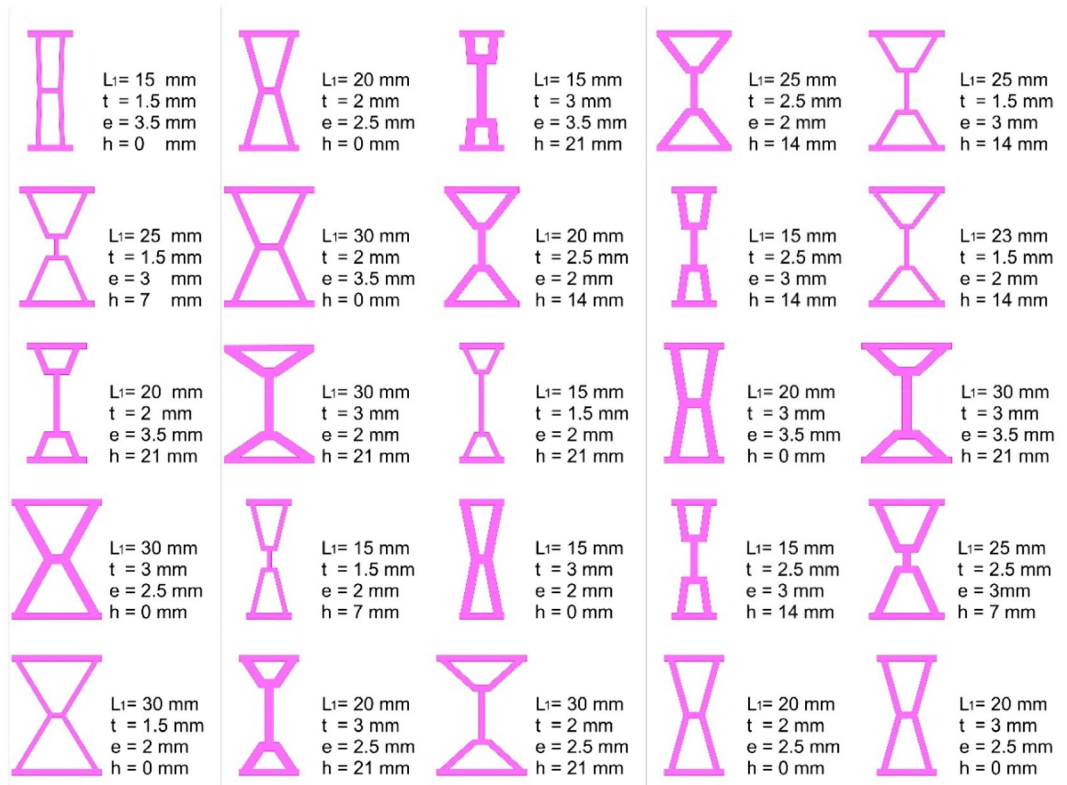


Figure 2. Configurations of the designed repetitive Y-shaped unit cells for the cores of the beams. Each configuration is characterized by different design parameters, including L_1 , t , e , and h , as indicated. These variations in parameters are to influence the mechanical responses of the beams under compressive loading conditions.

$$AE = X_{\text{Experiment}}^i - X_{\text{DFNNs}}^i \quad (1)$$

$$MAE = \frac{1}{n} \sum_{i=1}^n \left(X_{\text{Experiment}}^i - X_{\text{DFNNs}}^i \right) \quad (2)$$

$$MSE = \frac{1}{n} \sum_{i=1}^n \left(X_{\text{Experiment}}^i - X_{\text{DFNNs}}^i \right)^2 \quad (3)$$

$$R^2 = 1 - \frac{\sum_{i=1}^n \left(X_{\text{Experiment}}^i - X_{\text{DFNNs}}^i \right)^2}{\left(\overline{X_{\text{Experiment}}} - X_{\text{Experiment}}^i \right)^2} \quad (4)$$

Table 1. 3D-printing parameters.

| Parameter | Value |
|---------------------------|---------------------------|
| Number of contours | 3 |
| Raster direction | Alternating 45° per layer |
| Printing orientation | Flat on the print bed |
| Nozzle temperature | 215 °C |
| Bed temperature | 70 °C |
| Layer height | 0.15 mm |
| Printing speed | 50 mm min ⁻¹ |
| Material | White PLA+ |
| Diameter of the filaments | 1.75 mm |

3.2. Integration of ML-Oriented Regression and Classification

3.2.1. ML-Oriented Regression

The primary step in our methodology involves building a regression model to predict the properties of sandwich beams under

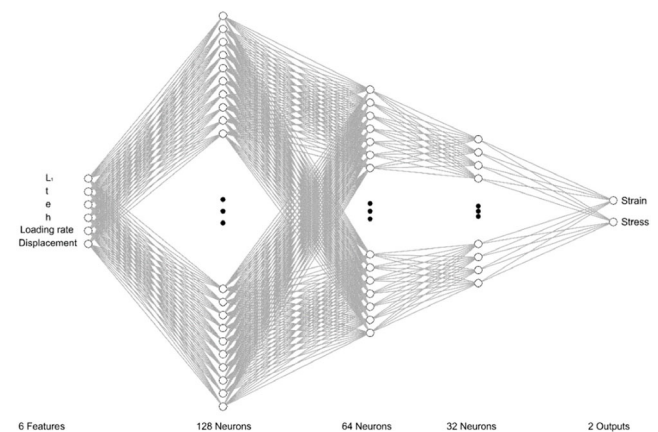


Figure 3. Architecture of the trained DFNN, holding six features (i.e., design parameters of the beams, loading rates, and induced compressive deformations during uniaxial compressive test), three hidden layers each comprising 128, 64, and 32 neurons, and two outputs (i.e., the resultant compressive strain and stress values).

compressive static and dynamic loading conditions. To achieve this, the XGBoost library in PYTHON was utilized, a powerful and efficient implementation of gradient-boosted decision trees.^[39–41] Initially, the design parameters of the beams (i.e., L_1 , t , e , and h), the loading crosshead speeds, and the induced compressive displacement were selected as inputs for the regression model. The outputs were the compressive properties of the beams (i.e., plateau stress, densification strain, densification stress, and compressive strength), critical indicators of the beams' mechanical performance. The dataset was preprocessed by normalizing the input and output data over the interval of [0-1]. The normalization values were saved for future use to ensure consistency in scaling. The normalized data was then split into training and validation sets using a 70–30 ratio. We employed a multioutput regressor with an XGBRegressor as the base estimator. Also, a grid search with cross-validation was conducted to identify the optimal hyperparameters for the model, which included the number of estimators, maximum depth, learning rate, subsample ratio, and column sample by tree ratio.

Finally, the model's performance was evaluated using metrics such as MSE, MAE, and the coefficient of determination. The results indicated the accuracy and reliability of the model in predicting the compressive properties of the beams and, afterward, the best model was used to generate predictions for a new dataset, comprising 6000 new samples within the interval of the design parameters. This expanded dataset provided a comprehensive understanding of the beams' behavior under three loading rates.

3.2.2. Classification

Following the regression analysis, a classification model was implemented to categorize the beams into static and dynamic classes. The classification problem was approached using support vector machines (SVMs) and decision tree algorithms. The training dataset included predictors such as the design parameters and mechanical properties of the beams. The response variable was the class label indicating whether the beam was subjected to static or dynamic loading. The training process involved a fivefold cross-validation to ensure the robustness of the models. Key performance metrics, including confusion matrix, MSE, accuracy score, and receiver operating characteristic (ROC) curve analysis, were used to assess the classifiers. The decision tree classifier, implemented with a bagging classifier to enhance its robustness, showed promising results with a high validation accuracy. The SVM, with a radial basis function or Gaussian kernel, was effective in handling the nonlinear boundaries between the static and dynamic classes.

In summary, the combination of regression and classification models provides a comprehensive framework for predicting and understanding the compressive response of novel symmetric Y-shaped core sandwich beams. This integrated approach leverages the strengths of both supervised learning techniques, enabling accurate predictions and effective categorization of the beams' behavior under various loading conditions. The methodologies and results presented in this study contribute significantly to the field of material science and engineering, presenting

a novel modeling scheme for the design and optimization of advanced engineering structures, especially 3D-printed sandwich beams.

4. Results and Discussion

4.1. DFNNs

The performance of the trained DFNN, which incorporates six input features and three hidden layers with 128, 64, and 32 neurons, respectively, along with two output neurons, was analyzed comprehensively. The trends of the MSE for the training, testing, and validation datasets were monitored throughout the training process, which concluded after 614 epochs. **Figure 4a** illustrates these trends, demonstrating a consistent decrease in MSE values across all datasets, indicative of the model's effective learning and convergence. Initially, the training error decreases rapidly before reaching a plateau, suggesting that the network is proficiently minimizing error on the training data. This rapid initial decrease indicates that the model quickly learns the fundamental patterns in the data, reducing large errors in the early stages of training, based on the backpropagation algorithm. The plateau phase suggests that the model fine-tunes its parameters to minimize error further, albeit at a slower rate. The validation error exhibits a similar trend, which is a strong indicator of the model's generalization capability. A similar trend in the validation error suggests that the model is concurrently memorizing the training data and learning patterns that generalize well to unseen data. Additionally, the testing error decreases in parallel with the training and validation errors, implying that the model is not overfitting and maintains robust performance on unseen data. The final MSE values are notably low ($\approx 1e-5$), which signifies high prediction accuracy. This low MSE indicates that the model predictions are very close to the actual values, reflecting the model's high fidelity.

The AE graph (Figure 4b) further elucidates the model's performance by displaying the AEs of the predictions. The AE values oscillate around zero with minimal variance, reflecting the minor differences between the predicted and actual values. This minimal variance in AE suggests that the model's predictions are consistently accurate across different samples. The MAE is remarkably low, recorded at $1.55e-5$, indicating that, on average, the predictions are exceedingly close to the actual values. This consistent pattern of low errors without significant spikes reinforces the model's accuracy. The low MAE value emphasizes that the average prediction error is minimal, showcasing the model's reliability and precision in making predictions. To further validate the DFNN's performance, a linear regression analysis of the predictions versus the actual values was conducted. This is visualized in Figure 4c, where the scatter plot illustrates the relationship between the compressive responses predicted by the DFNN and the experimental values, showcasing a strong linear correlation with a coefficient of determination ($R^2 = 0.999$). This high R^2 value underscores the model's accuracy in predicting the experimental outcomes. The overall linear trend in the data aligns with expectations based on the mechanical properties of the Y-shaped core sandwich beams. Minor deviations from the line of best fit can be attributed to natural variability inherent

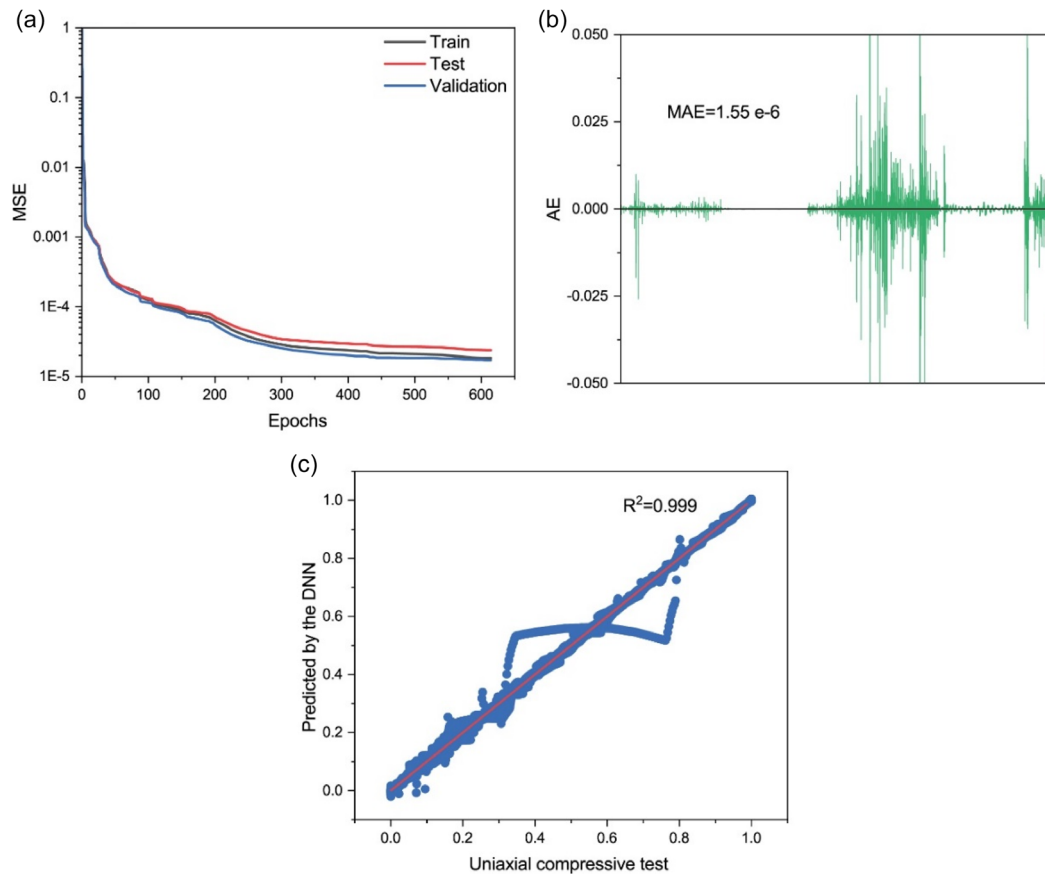


Figure 4. Results of the trained DFNN: a) trend of the MSE over the training process for train, test, and validation data, b) calculated AE between the predicted values and experimental data, and c) depiction of the predicted values of strain and stress versus the data obtained from uniaxial compressive tests.

in experimental conditions. These include slight inconsistencies in the 3D-printing process, potential material inhomogeneity, and the resolution limits of the testing equipment during compressive tests.^[42–46] The variations are common in experimental studies and do not indicate irregularities or limitations in the predictive model. These findings further validate the reliability of the DFNN in capturing the compressive behavior of the beams.

In summary, the near-perfect linear relationship and the high R^2 value confirm that the DFNN model accurately predicts the compressive response of the beams. The MSE, AE, and accurately predicts the compressive response of the beams. The metrics collectively demonstrate the model's robustness and reliability. The low MSE and MAE values indicate minimal prediction errors, while the high R^2 value showcases the model's ability to explain almost all the variance in the actual values. These results highlight the DFNN's effectiveness in capturing the complex relationships in the data, making it a powerful tool for predicting the compressive response of novel symmetric Y-shaped core sandwich beams.

In the next step of assessing the trained DFNN's performance, mechanical responses of the beams underwent experimental static and dynamic compressive deformations were plotted juxtapose compressive stress–strain curves the predicted by the DFNN. From **Figure 5**, it is seen that the trained DFNN was

capable of predicting the beams compressive response under both static and dynamic loading conditions, further proving the previous discussions of the metrics, by which the trained DFNN could be trusted for predicting the Y-shaped core beams' compressive responses. Based on the stress–strain plots represented in **Figure 5**, it was seen that the design parameters of the beams affected the beams response. In all the plots of **Figure 5**, three regions of linear, plateau, and densification were seen. Over the linear region, the initial part of the curves representing the elastic behavior of the structures, stress increases linearly with strain. Following the linear region, the second phase of the curves, plateau region, shows a more gradual increase in stress, indicating energy absorption through progressive deformation. Lastly, densification point, where the curve rises steeply again, indicates that the structure is fully compacted, and further deformation results in a significant and sharp increase in stress.

As mentioned in Section 2, four design parameters of L_1 , t , e , and h , all in millimeters, were considered in Design Expert software. Accordingly, we aimed to investigate these parameters and their effects on the beams' mechanical responses. The first parameter that was investigated on the beams static and dynamic behavior was L_1 . Observations indicate that as L_1 increases, the stiffness of the beam also increases, leading to a steeper slope in the linear region. This is evident in the graphs where beams with

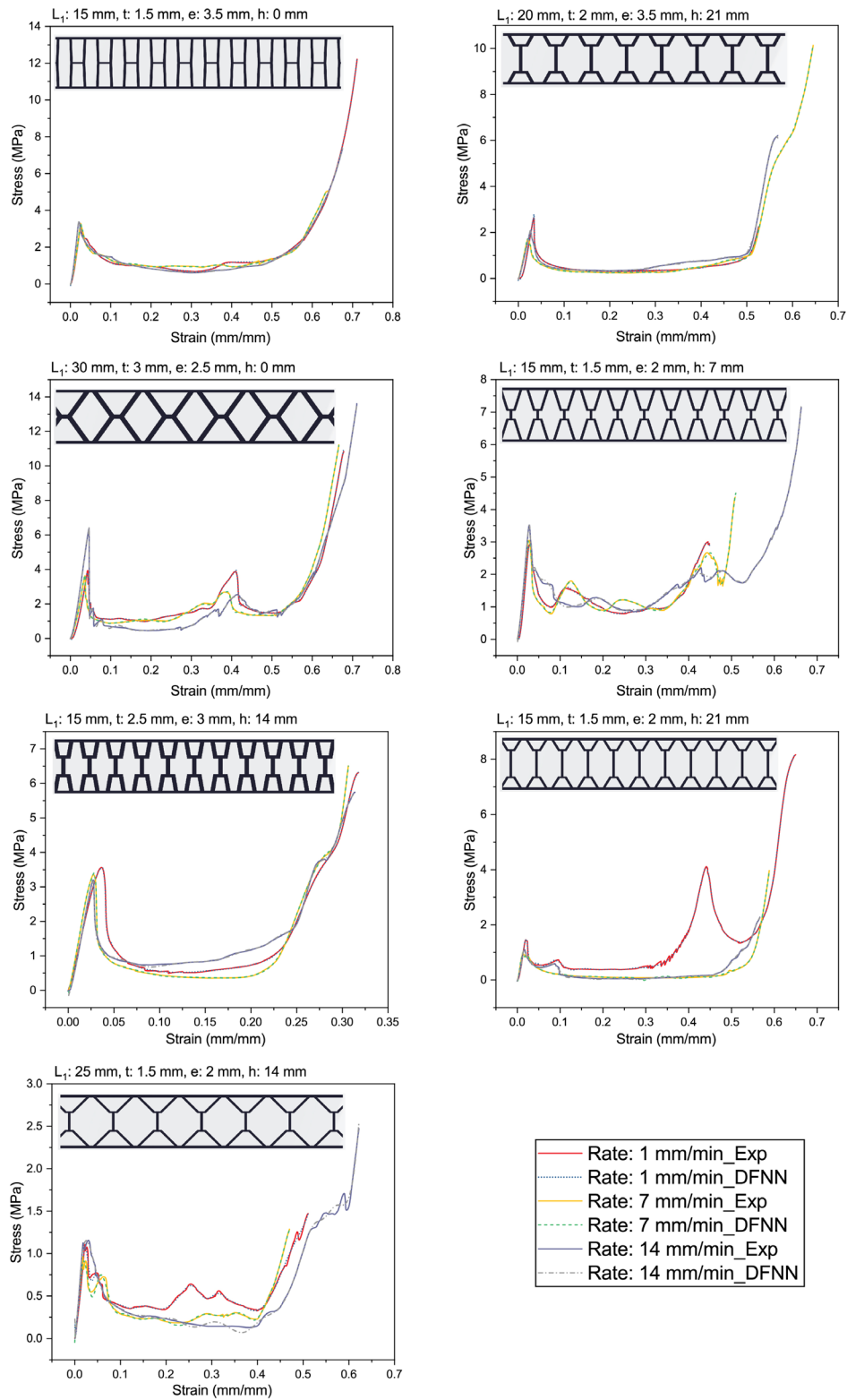


Figure 5. Experimental and predicted stress–strain curves for the beams under both static and dynamic loading conditions. Each subplot represents a different beam geometry, with variations in L_1 , t , e , and h , as shown. The legend differentiates between experimental results (Exp) and DFNN predictions at various loading rates (i.e., 1, 7, and 14 mm min⁻¹).

$L_1 = 30$ mm exhibit higher initial stiffness compared to those with $L_1 = 15$ mm. The thickness (i.e., the t parameter) also plays a significant role, the beams with thicker Y-shaped core unit cells (e.g., $t = 3$ mm) showing higher stiffness compared to thinner beams, in which $t = 1.5$ mm. The edge thickness (e) and height (h) influence the stiffness in a more nuanced manner, contributing to the overall stability and load distribution. The plateau region signifies the post-yield behavior where the beams undergo plastic deformation. Beams with larger L_1 values tend to have a more extended plateau, indicating higher energy absorption capacity. The h parameter particularly in designs with significant heights (e.g., $h = 21$ mm) shows a noticeable effect on the plateau length and stress levels. For instance, beams with higher h parameter exhibit prolonged plateaus at higher stress levels. Additionally, variations in t and e also impact the plateau, where increased thickness generally contributes to a higher plateau stress. In contrast, the strain values at which densification initiates are influenced by all four parameters. Beams with larger L_1 and h values typically reach the densification point at higher strains, indicating that these beams can undergo more deformation before densification.

Other than the design parameters, which were proved to affect the mechanical response of the beams, in this study, we dealt with another variable, which was considered after design of the samples. Loading rate (1, 7, and 14 mm min^{-1}), the parameter showed up in experimental tests conducted on the 3D-printed samples, significantly impacts the onset of densification. At higher rates (e.g., 14 mm min^{-1}), the densification starts earlier due to the increased inertia effects and reduced time for structure relaxation. The loading rate substantially affects all regions of the stress-strain curve. At higher loading rates (14 mm min^{-1}), the beams exhibit higher stress levels throughout the entire curve compared to lower rates (1 mm min^{-1}). This could be related to the rate-dependent behavior of the structures, where higher rates induce elevated stress due to inertia and strain rate sensitivity. Overall, the compressive response of Y-shaped core sandwich beams is considerably dependent on the design parameters L_1 , t , e , and h , as well as the loading rates adopted during the conducted uniaxial compressive tests. Larger values of L_1 and h contribute to increased stiffness, prolonged plateau regions, and higher densification points, enhancing the total energy absorption capacity. The loading rate influences the stress levels and the onset of densification, with higher rates resulting in increased stresses and earlier densification.

4.2. Integration of ML-Oriented Regression and Classification

After training the DFNNs, a Python code was developed to create a scheme for predictive modeling of the beams' compressive properties. Implementing the ISO 13 314:2011 standard, four major properties of the beams (i.e., plateau stress, densification strain, densification stress, and compressive strength) were obtained under both static and dynamic loading conditions. These compressive properties, loading rates, and the geometric features of the Y-shaped cores of the beams were analyzed by solving a regression problem using the XGBoost library in Python, a powerful supervised learning platform. The regression analysis yielded an MAE of 0.0244, MSE of 0.0047, and R^2 of

0.93, indicating high predictive accuracy without overfitting. Subsequently, 18 000 new samples were generated, and their compressive properties were predicted using the trained model. These predicted properties were then classified into two categories of static and dynamic, based on the loading rate imposed on the beams. This classification was performed using SVM with a radial basis function and decision tree algorithms. Specifically, a loading rate of 1 mm min^{-1} was designated as the static class, while loading rates of 7 and 14 mm min^{-1} were categorized as the dynamic class.

Accordingly, the performance of the decision tree and SVM classifiers for predicting the compressive response of symmetric Y-shaped core sandwich beams were thoroughly evaluated, and a detailed comparison and analysis of the results obtained from these two classifiers have been presented in this subsection. To elaborate, the classification performance of the two supervised learning algorithms, decision tree and SVM, was assessed using confusion matrices, ROC curves, and various metrics such as precision, recall, F1 score, MSE, and accuracy, see Table 2 and 3.

The decision tree algorithm exhibited exceptional performance across all metrics, indicating its robustness in distinguishing between dynamic and static categories. The confusion matrix in Figure 6a reveals very high true positive rates for both dynamic and static categories. There were minimal misclassifications, demonstrating the decision tree's effectiveness in correctly classifying the majority of instances. The precision, recall, and F1 score for the dynamic category were 0.9979, 0.9990, and 0.9984, respectively. Similarly, for the static category, these values were 0.9980, 0.9958, and 0.9969. These high values indicate that the model is both precise and sensitive, accurately identifying most positive cases while minimizing false positives and false negatives.

The MSE for both validation and the overall dataset is low (0.0021), reinforcing the model's accuracy and low error rate. Also, the overall accuracy stands at 99.79%, reflecting the

Table 2. Detailed report of the classification problem solved employing decision tree algorithm.

| | Precision | Recall | F1 score | Support | MSE | Validation accuracy |
|------------------|-----------|--------|----------|---------|--------|---------------------|
| Dynamic | 0.9979 | 0.9990 | 0.9984 | 12 042 | 0.0021 | 0.9978 |
| Static | 0.9980 | 0.9958 | 0.9969 | 6021 | 0.0021 | 0.9978 |
| Macro average | 0.9979 | 0.9974 | 0.9976 | 18 063 | 0.0021 | 0.9978 |
| Weighted average | 0.9979 | 0.9979 | 0.9979 | 18 063 | 0.0021 | 0.9978 |

Table 3. Report of assessment metrics of the classification done utilizing the SVM.

| | Precision | Recall | F1 score | Support | MSE | Validation accuracy |
|------------------|-----------|--------|----------|---------|--------|---------------------|
| Dynamic | 0.7712 | 0.8911 | 0.8268 | 12 042 | 0.2489 | 0.7512 |
| Static | 0.6839 | 0.4711 | 0.5579 | 6021 | 0.2489 | 0.7512 |
| Macro average | 0.7276 | 0.6812 | 0.6924 | 18 063 | 0.2489 | 0.7512 |
| Weighted average | 0.7421 | 0.7512 | 0.7372 | 18 063 | 0.2489 | 0.7512 |

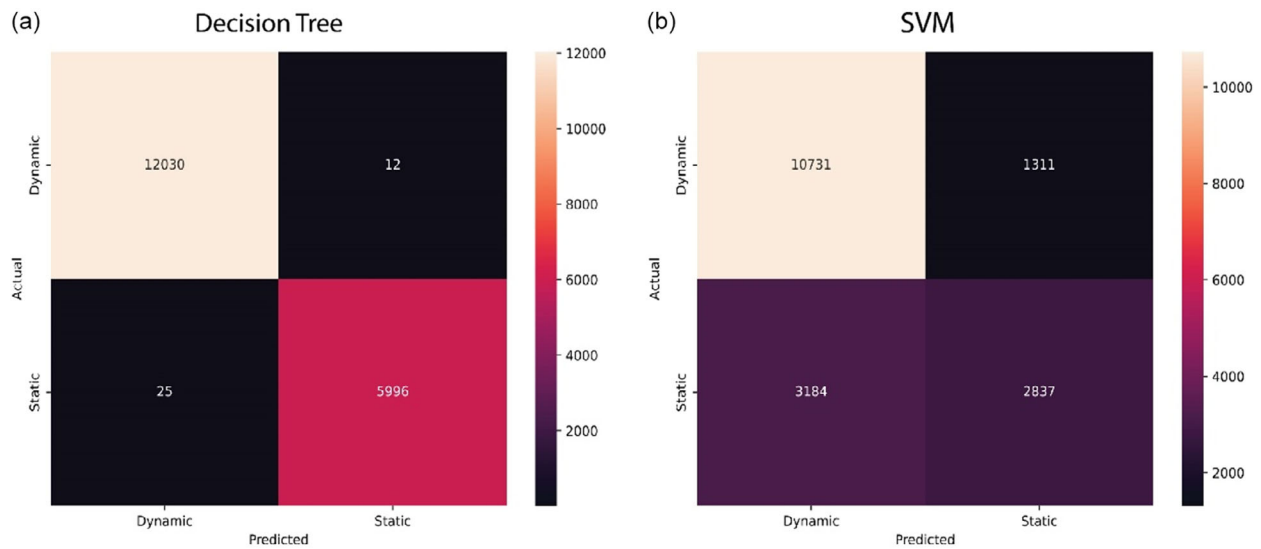


Figure 6. Confusion matrices for the two classifiers: a) decision tree and b) SVM. The decision tree classifier demonstrates a significantly lower number of misclassifications compared to the SVM classifier, indicating higher reliability.

model's outstanding performance in correctly predicting the labels for the majority of the instances. The macro and weighted averages for precision, recall, and F1 score are similarly high, signifying that the model performs consistently well across both categories and that the performance is balanced irrespective of class distribution. The high metrics and low error rates confirmed that the decision tree algorithm was highly reliable and effective for this classification of the 3D-printed sandwich beams' behavior into two classes of static and dynamic.

In contrast, the SVM algorithm showed moderate performance, which indicates room for improvement compared to the decision tree, compare Figure 6a and b. The confusion matrix for the SVM algorithm indicates a higher number of misclassifications compared to the decision tree. The true positive rates of dynamic and static categories were lower, suggesting the model struggled more with accurately classifying instances. For the dynamic category, the precision, recall, and F1 score were 0.7712, 0.8911, and 0.8268, respectively. Also, for the static category, these metrics were lower at 0.6839, 0.4711, and 0.5579. These results suggest that the SVM model had difficulty in balancing precision and recall, particularly for the static category. Meanwhile, the MSE is significantly higher at 0.2489, indicating a higher error rate and lower prediction accuracy compared to the decision tree. The overall accuracy of the SVM algorithm is 75.12%, which, while moderate, is substantially lower than that of the decision tree. The macro and weighted averages for precision, recall, and F1 score reflect the model's uneven performance across categories. The lower metrics indicate that the SVM model's predictions were less consistent and reliable, and the moderate performance of the SVM algorithm suggests that it may not be as well-suited for this specific classification task as the decision tree. The relatively lower precision, recall, F1 score, and higher MSE indicate that the SVM model did not possess the ability of effective distinguishing between dynamic and static categories.

As the latest metric in assessing the classifiers' performance, we focused on the ROC curves and the area under the curve (AUC), providing additional insights into the classification performance of both models. The ROC curves for the decision tree show that it achieves high true positive rates across various threshold settings, with the AUC likely close to 1. This further confirms the model's excellent discriminative ability. The ROC curves for the SVM suggest more moderate true positive rates, with a lower AUC compared to the decision tree. This aligns with the observed lower precision, recall, and F1-score metrics, reported in Table 1 and 2, as well as the confusion matrices in Figure 6 and 7.

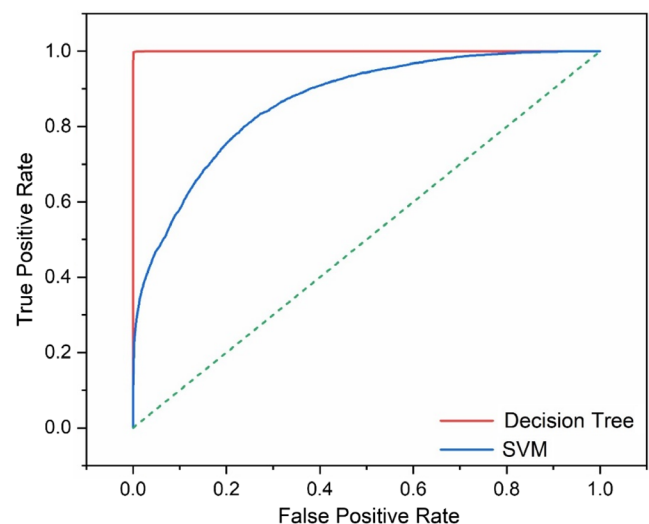


Figure 7. ROC curves for the decision tree and SVM classifiers. The decision tree classifier shows superior performance with a higher true positive rate and a lower false positive rate compared to the SVM classifier, indicating better overall classification accuracy.

As a concluding remark on the second supervised learning scheme, in which regression and classification were integrated for predictive modeling of the 3D-printed sandwich beams with Y-shaped cores, the decision tree algorithm demonstrates superior performance in classifying dynamic and static categories, with high precision, recall, F1 score, accuracy, and low MSE. The SVM algorithm, while moderately effective, shows lower performance across these metrics and higher error rates. These findings suggest that for this specific classification task, the decision tree algorithm is more reliable and accurate compared to the SVM algorithm. Further improvements to the SVM model or alternative algorithms may be explored to enhance classification performance.

5. Conclusion

In conclusion, this study demonstrated the application of DFNNs in predicting the compressive response of novel Y-shaped core sandwich beams. The accuracy of the DFNN model, as validated by experimental data, confirmed its effectiveness in modeling the complex stress-strain curves under both static and dynamic loading conditions. The investigation into key design parameters (i.e., L_1 , t , e , and h) revealed their considerable influence on the mechanical response, particularly in the linear, plateau, and densification regions of the stress-strain curves. Higher values of L_1 and h were found to enhance stiffness, extend plateau regions, and delay the onset of densification, thereby increasing the energy absorption capacity of the beams. Additionally, the study highlighted the significant effect of loading rates, with higher rates leading to earlier densification and increased stress levels due to inertia effects and reduced relaxation time. The decision tree algorithm outperformed the SVM in classifying dynamic and static loading conditions, achieving an accuracy of 99.79%. The design and optimization of sophisticated sandwich structures has thus benefited greatly from these predictive modeling schemes, which may find use in engineering applications such as construction, automotive, and aerospace where exact mechanical performance, lightweight materials, and energy absorption capabilities are essential.

Acknowledgements

This research was supported by Basic Science Research Program through the National Research Foundation of Korea (NRF) funded by the Ministry of Education (grant no.: 2018R1A6A1A03024509) and the RAEng/Leverhulme Trust Research Fellowship (award no.: LTRF-2324-20-129).

Conflict of Interest

The authors declare no conflict of interest.

Author Contributions

Ali Khalvandi: conceptualization (equal), data curation (lead), investigation (equal), methodology (equal), software (lead), and writing—original draft (lead); **Saeed Kamarian:** conceptualization (lead), investigation (equal), methodology (equal), project administration (lead), and writing—review and editing (equal); **Mahdi Bodaghi:** conceptualization

(equal), investigation (equal), methodology (equal), validation (equal), and writing—review and editing (equal); **Saeed Saber-Samandari:** investigation (equal), methodology (equal), supervision (equal), and writing—review and editing (equal); and **Jung-il Song:** funding acquisition (lead); investigation (equal); supervision (lead); and writing—review editing (equal).

Data Availability Statement

The data that support the findings of this study are available from the corresponding author upon reasonable request.

Keywords

3D-printed sandwich beams, decision trees, deep feed-forward neural networks, regressions, support vector machines, Y-shaped unit cells

Received: September 13, 2024

Revised: November 22, 2024

Published online:

- [1] D. Zenkert, *An Introduction to Sandwich Structures*, Student Edition, DTU Mechanical Engineering, Technical University of Denmark, Lyngby, Denmark **1995**.
- [2] V. Birman, G. A. Kardomateas, *Composites, Part B* **2018**, *142*, 221.
- [3] V. Patekar, K. Kale, *Polym. Compos.* **2022**, *43*, 5820.
- [4] S. K. Sahu, P. R. Sreekanth, S. K. J. P. Reddy, *Polymers* **2022**, *14*, 4267.
- [5] Q. Ma, M. Rejab, J. Siregar, Z. Guan, *J. Compos. Mater.* **2021**, *55*, 2513.
- [6] T. Khan, V. Acar, M. R. Aydin, B. Hülägü, H. Akbulut, *Polym. Compos.* **2020**, *41*, 2355.
- [7] R. Barbaz-Isfahani, A. Khalvandi, T. Mai Nguyen Tran, S. Kamarian, S. Saber-Samandari, J.-I. Song, *Ind. Crops Prod.* **2023**, *205*, 117498.
- [8] V. T. Le, N. S. Ha, N. S. Goo, *Composites, Part B* **2021**, *226*, 109301.
- [9] A. W. Alshaer, D. J. Harland, *Compos. Struct.* **2021**, *257*, 113391.
- [10] M. F. Aly, K. T. Hamza, M. M. Farag, *Mater. Des.* **2014**, *56*, 219.
- [11] M. Abu-Saleem, J. M. Gattas, *Eng. Struct.* **2024**, *305*, 117678.
- [12] K. F. Karlsson, B. TomasAström, *Composites, Part A* **1997**, *28*, 97.
- [13] T. D. Ngo, A. Kashani, G. Imbalzano, K. T. Nguyen, D. Hui, *Composites, Part B* **2018**, *143*, 172.
- [14] S. Kamarian, A. Khalvandi, E. Heidarzadi, S. Saber-Samandari, J.-I. Song, *Int. J. Mech. Sci.* **2024**, *262*, 108747.
- [15] A. A. Bakır, R. Atik, S. Özerinç, *Rapid Prototyping J.* **2021**, *27*, 537.
- [16] S. Wickramasinghe, T. Do, P. J. P. Tran, *Polymers* **2020**, *12*, 1529.
- [17] P. Qiao, M. Yang, *Composites, Part B* **2007**, *38*, 739.
- [18] B. Russell, T. Liu, N. Fleck, V. S. Deshpande, *Int. J. Impact Eng.* **2012**, *48*, 65.
- [19] C. Betts, *Mater. Sci. Technol.* **2012**, *28*, 129.
- [20] N. Wicks, J. W. Hutchinson, *Mech. Mater.* **2004**, *36*, 739.
- [21] M. Brendon Francisco, J. Luiz Junho Pereira, S. Simões da Cunha, G. Ferreira Gomes, *Eng. Struct.* **2023**, *281*, 115775.
- [22] M. B. Francisco, J. L. J. Pereira, A. P.d. Paiva, E. L. Barbedo, S. S. da Cunha Jr, G. F. Gomes, *Mech. Adv. Mater. Struct.* **2023**, *31*, 8058.
- [23] G. E. Dieter, *Mechanical Behavior under Tensile and Compressive Loads*, ASM International **2000**, pp. 99–108.
- [24] A. Khalvandi, M. M. Aghdam, S. Saber-Samandari, *27th National and 5th Int. Iranian Conf. on Biomedical Engineering (ICBME)*, Tehran, Iran, November **2020**, pp. 163–167.

- [25] A. Khalvandi, M. Mohammadi Aghdam, S. Saber-Samandari, *Proc. Inst. Mech. Eng., Part N* **2022**, 236, 117.
- [26] S. Kamarian, A. Teimouri, M. Alinia, S. Saber-Samandari, J. I. Song, *Polym. Compos.* **2024**, 45, 3043.
- [27] A. Khalvandi, S. Saber-Samandari, M. M. Aghdam, *Biomater. Adv.* **2022**, 136, 212768.
- [28] R. Chen, W. Zhang, X. J. A. Wang, *Atmosphere* **2020**, 11, 676.
- [29] M. Sharifzadeh, A. Sikinioti-Lock, N. J. R. Shah, S. E. Reviews, *Renewable Sustainable Energy Rev.* **2019**, 108, 513.
- [30] A. Karpatne, I. Ebert-Uphoff, S. Ravela, H. A. Babaie, V. Kumar, *IEEE Trans. Knowl. Data Eng.* **2018**, 31, 1544.
- [31] V. M. Krasnopolsky, M. S. Fox-Rabinovitz, *Neural Networks* **2006**, 19, 122.
- [32] G. D. Goh, S. L. Sing, W. Y. Yeong, *Artif. Intell. Rev.* **2021**, 54, 63.
- [33] A. Ali, R. D. Riaz, U. J. Malik, S. B. Abbas, M. Usman, M. U. Shah, I.-H. Kim, A. Hanif, M. Faizan, *Materials* **2023**, 16, 4149.
- [34] X. Sun, K. Zhou, F. Demoly, R. R. Zhao, H. J. Qi, *J. Appl. Mech.* **2023**, 91, 030801.
- [35] G. D. Goh, W. Y. Yeong, *Mater. Today: Proc.* **2022**, 70, 95.
- [36] U. Demircioğlu, A. Sayil, H. Bakir, *Arabian J. Sci. Eng.* **2024**, 49, 1611.
- [37] A. Khalvandi, S. Saber-Samandari, M. M. Aghdam, *Heliyon* **2024**, 10, e28995.
- [38] Y. Wang, L. Lu, H. Song, *IOP Conf. Ser.: Mater. Sci. Eng.* **2019**, 563, 042028.
- [39] N. M. Shahani, M. Kamran, X. Zheng, C. Liu, X. Guo, *Adv. Civ. Eng.* **2021**, 2021, 2565488.
- [40] C. N. Obiora, A. Ali, A. N. Hasan, in *2021 IEEE PES/IAS PowerAfrica*, IEEE **2021**, pp. 1–5.
- [41] T. Chen, C. Guestrin, in *Proc. of the 22nd ACM Sigkdd Int. Conf. Knowledge Discovery and Data Mining* **2016**, pp. 785–794.
- [42] N. Vidakis, M. Petousis, N. Mountakis, A. Korlos, V. Papadakis, A. Moutsopoulou, *J. Funct. Biomater.* **2022**, 13, 115.
- [43] P. D. Nguyen, T. Q. Nguyen, Q. B. Tao, F. Vogel, H. J. V. Nguyen-Xuan, *Virtual Phys. Prototyping* **2022**, 17, 768.
- [44] M. Petousis, N. Vidakis, N. Mountakis, E. Karapidakis, A. Moutsopoulou, *Polymers* **2023**, 15, 1232.
- [45] I. Rojek, D. Mikołajewski, P. Kotlarz, M. Macko, J. Kopowski, *Bulletin of the Polish Academy of Sciences* **2021**, 69, e136722.
- [46] M. M. Shirmohammadi, S. J. Goushchi, P. M. Keshtiban, *Prog. Addit. Manuf.* **2021**, 6, 199.